Catalysis Today 213 (2013) 183–191

Contents lists available at SciVerse ScienceDirect

Catalysis Today

journal homepage: www.elsevier.com/locate/cattod

Cu, Ce/mordenite coatings on FeCrAl-alloy corrugated foils employed as catalytic microreactors for CO oxidation

Nicolás C. Pérez, Eduardo E. Miró, Juan M. Zamaro*

Instituto de Investigaciones en Catálisis y Petroquímica, INCAPE (FIQ, UNL CONICET) Santiago del Estero 2829, 3000 Santa Fe, Argentina

ARTICLE INFO

Article history:
Received 1 November 2012
Received in revised form 7 February 2013
Accepted 11 February 2013
Available online 30 March 2013

Keywords:
Film growth
Zeolite coating
FeCralloy
Microreactor
CO oxidation

ABSTRACT

The aim of this work was to study different strategies for the synthesis of mordenite coatings on thin FeCrAl alloy foils in order to obtain adherent, stable and homogeneous films for their use as catalytic microreactors. For this purpose, the substrate pretreatments and growth conditions of the films by secondary synthesis were investigated. The best results were obtained by applying a brief calcination of the foils at 700 °C that developed a smooth alumina film with hydrophilic properties, followed by immersion in a 0.4 wt.% aqueous solution of the cationic polymer poly-(diallyldimethilammoniumchloride), PDDA. The subsequent seeding with diluted nanocristal suspensions (2 g L) of Na-mordenite allowed the development of zeolite films with the desired properties and the additional benefit of a marked preferential growth on the metallic surface at the expense of a negligible growth within the synthesis solution. Finally, homogenous zeolite films were obtained in micro-corrugated foils, after which Cu and Ce were incorporated as catalytic ingredients and used in a microreactor for the CO oxidation reaction under different conditions.

1. Introduction

Microreactors are structured catalysts with channels in the micrometer range that have exceptional advantages with respect to conventional reactors due to the higher heat and mass transfer rates they can achieve [1]. The most widely reported supports to build these devices are bulk plates of millimetric thickness made of silicon and stainless steel with microchannels [2]. However, the use of thin foils of metallic substrates could bring about certain advantages, i.e. the possibility of achieving both thin catalytic walls with high mechanical resistance and different configurations in shape and size of the microchannels. Zeolites are interesting materials to be used in catalysis because they can be employed in a broad variety of reactions; they also show high thermal stability and reproducibility of synthesis. However, the number of publications reporting an effective catalytic application of zeolite-based microreactors is still limited [3–10].

The FeCrAl stainless steel (FeCralloy®) is an appropriate material to be used as catalytic support because it can form a thin superficial alumina film [11]. This type of substrate has been employed for the in situ growth of crystalline zeolite coatings [12,13] and also for the preparation of zeolite-based structured catalysts with millimetric channels [14,15]. A key factor is the obtention of thin, uniform and adherent zeolite films in the microchannels, which should be smaller than 500 μm. On the other hand, the secondary synthesis method has been shown to be a good means of obtaining homogeneous zeolite coatings because it skips the nucleation step onto the support surface and can also yield different film characteristics [16]. Key variables of this method are seed concentration and seed size, which can lead to different film microstructures and crystallographic orientations, attributed to a competitive growth process [17]. However, the zeolite synthesis inside the microchannels in closed configuration could originate the formation of non-homogeneous coatings with unstable over-growths, product of diffusive limitations of the nutrients to the microchannels. In order to avoid this problem, an alternative is to carry out the zeolite film growth in open microchannels after which microreactors can be built by stacking the coated microchannelled foils.

In this work, we studied the effect of the conditions of the secondary synthesis method on the physicochemical properties of mordenite coatings in order to obtain stable, homogeneous and well-ordered films onto microchannelled FeCralloy foils. After the coating optimization, Cu and Ce were added as active elements into the films which were successfully applied as microreactors in the CO oxidation reaction.

2. Experimental

2.1. Materials and pretreatments

FeCralloy® (Goodfellow) foils of 50 μm thick were employed as the support material for the zeolite growth. They were cut in pieces

* Corresponding author. Tel.: +55 0342 4536861; fax: +55 0342 4536861.
E-mail addresses: zamaro@fiq.unl.edu.ar, jmzamaro@gmail.com (J.M. Zamaro).

0920-5861/$ – see front matter © 2013 Elsevier B.V. All rights reserved.
http://dx.doi.org/10.1016/j.cattod.2013.02.014

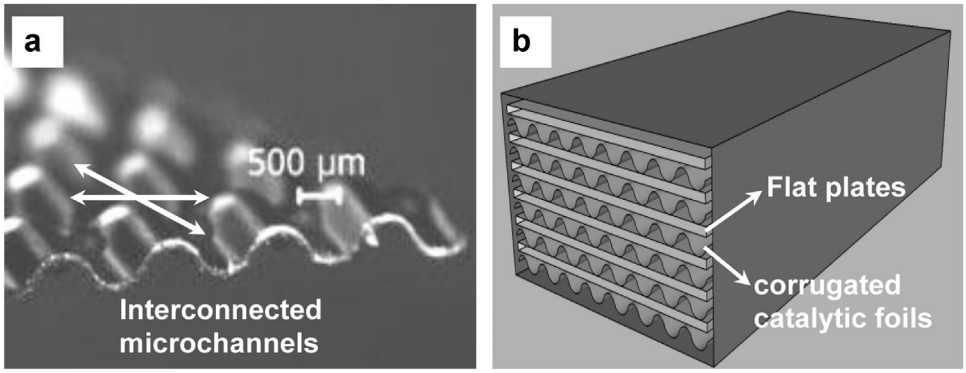

Fig. 1. (a) Detail of a microcorrugated foil with interconnected microchannels and (b) scheme of the microreactor assembly in a stacked-foil configuration.

of 2 cm × 1 cm and some of them were micro-corrugated employing a home-made device so as to obtain interconnected microchannels (see Fig. 1a). This type of geometry can increase the turbulence inside the channels as already reported [18]. Foils were thoroughly cleaned with a brush first with soap and water and then with acetone; then, they were subjected to ultrasound for 5 min alternately in the same solvents. After that, the foils were calcined in air either at 700 °C for 1 h or at 900 °C for 22 h. In the case in which calcinations were conducted at the lower temperature, the treated foils were submerged in a 0.4 wt.% aqueous solution of the low molecular weight cationic polymer poly-(diallyldimethilammoniumchloride) (PDDA) Aldrich, during 20 min and then washed with distilled water.

2.2. Seeding process and zeolite film growth

The pretreated supports were seeded using 2–10 g L^{-1} nanocrystal suspensions (200 nm) made of commercial mordenite crystals obtained from different sources: Na-mordenite Zeolyst, Na-mordenite Valfor C500-11 from the PQ Corporation, H-mordenite Zeolon and a dealuminated H-mordenite. The nanometric seeds were obtained from the supernatant after centrifuging suspensions of the as received powders at 3500 rpm for 30 min. Using this procedure, suspensions of nanocrystals sized about 200 nm were obtained, as previously determined by LPSA [19]. The seeding of the supports treated with PDDA was performed by contacting the foils with the nanocrystal suspensions during 20 min. After that, the foils were cleaned with distilled water. On the other hand, the seeding of the foils that were not treated with PDDA was performed by dip-coating, placing the supports inside a burette filled with the suspension and emptying it dropwise at a 1 cm min^{-1} velocity. Afterwards, all samples were dried in air for 30 min and then in a stove for 15 min at 120 °C.

For the film growth, the seeded foils were submerged into a gel made of SiO_2 (Ludox® AS 40), $Na_2Al_2O_4$ (Riedel-de-Haen) and NaOH (Cicarelli pro-analysis) with a Na_2O:Al_2O_3 ratio of 0.38:0.025 and H_2O:SiO_2 ratios from 70:1.15 to 210:1.15. Template agents were not employed. The hydrothermal treatments were performed at 180 °C between 3 and 24 h, after which the autoclave was cooled and the samples were withdrawn, vigorously washed with a brush under water and afterwards treated in an ultrasonic bath for 10 min to remove residues from the solution. The solids produced within the solution were also recovered. Finally, all the samples were dried in a stove at 120 °C overnight.

2.3. Addition of active metals to the zeolite coatings

Cu ions were introduced in zeolite layers by ionic exchange using a 0.01 M aqueous solution of $Cu(NO_3)_3$ under stirring at room temperature and pH 5 during 24 h. After the exchange, the coatings were washed with distilled water and dried; they were later impregnated with Ce by dip-coating with a colloidal CeO_2 commercial suspension (Nyacol®, 20 wt.% in acetate). The Cu,Ce/zeolite coated foils were finally calcined in air to 400 °C for 2 h in order to decompose the nitrate and acetate precursors.

2.4. Characterization techniques

Through X-ray diffraction (XRD), it was possible to identify the crystalline phases of the crystals produced on the supports and within the synthesis solution. A Shimadzu XD-D1 instrument operated at 40 kV and 30 A was employed with a scanning rate of 2° min^{-1} between 2θ = 5–40°. The diffraction patterns obtained were compared to those of pure mordenite powders. Furthermore, the diffraction data were used to identify crystallographic preferential orientations. Scanning electron microscopy (SEM) was used to determine the microstructure and the spatial ordering of the crystals in the growths. To do so, a SEM Jeol JSM-35C instrument was employed operated at 20 kV. The samples were glued to the sample holder with Ag painting and due to the low electrical conductivity of the zeolite, they were then coated with a thin layer of Au in order to improve the images. A dispersive EDAX instrument coupled to the SEM was employed to perform the electron probe micro analysis (EPMA) of the films. Analyses were performed at different depths in the film thickness in cross-sections of the samples so as to obtain the composition profiles.

2.5. Catalytic evaluations of microreactors

The FeCrAl alloy microcorrugated foils coated with Cu,Ce/mordenite films were stacked inside a module of 1 cm × 1 cm section and 2 cm long, placing six catalytic foils between flat stainless-steel plates as shown in Fig. 1b. Prior to the catalytic evaluation, the microreactors were treated in air (50 mL min^{-1}) between room temperature and 400 °C at 5 °C min^{-1}, and maintained at that temperature for 1 h. After that, the catalytic runs were performed using a gas feed composed of 1% CO, 2–20% O_2 in He balance. The total flow was varied between 20 and 40 cm^3 min^{-1} (flow/mass ratio between 600 and 300 cm^3 min^{-1} g^{-1}). The CO conversions were determined by analyzing the reactor exit with an on-line Shimadzu GC-2014 cromatograph equipped with a TCD detector and a 5A molecular sieve column.

3. Results and discussion

3.1. Synthesis of zeolite coatings on supports calcined at 900 °C

3.1.1. Temporal evolution of zeolite films

The samples prepared in this series of experiments were designed as F900 and are presented in Table 1. These samples

Table 1
Syntheses performed onto FeCralloy foils calcined at 900 °C.

Sample	Synthesis time (h)	Seeding suspension ($g\,L^{-1}$)	Weight gain (%)
F900-1	3	5	0.3
F900-2	6	5	1.5
F900-3	24	5	14.3
F900-4	24	10	8.4
F900-5	24	2	19.4

were prepared by seeding with Zeolyst Na-mordenite nanocrystals. In agreement with the data reported in the literature [11], alumina whiskers were produced in the foils calcined at 900 °C for 22 h. These whiskers can serve to effectively anchor the nanocrystal seeds. However, some inhomogeneities can be observed in the seed distribution, originated in the somewhat non-uniform growth of the alumina whiskers (Fig. 3e). After the hydrothermal treatments, growths of mordenite were obtained in all samples as indicated by their respective XRD diffraction patterns (Fig. 2). Note that all the diffraction signals obtained for the powder collected after synthesis coincide with those of the mordenite structure. During the temporal sequence (F900-1–F900-3) the mordenite loading increased with time, in line with its increased XRD intensities (Fig. 2). When the synthesis treatment was performed for 3 h, although the mass produced was poor (Table 1) and the zeolite XRD signals could not be observed, the SEM picture (Fig. 3a) depicted an incipient growth around the seeded crystals. Moreover, the whisker structures were no longer observed, whereas a smooth surface could be observed on which the seeded crystals grew. These transformations were due to a partial dissolution of the surface whiskers due to the strong basic medium and to the formation of a gel-like film during the synthesis process, respectively. The formation of a gel layer on a support surface during the synthesis of zeolite films is a recognized phenomenon in which the crystallization is produced within the said amorphous layer [20,21] promoted by the seed crystals that provide nucleation sites on the surface [22]. At higher magnification, it can be noticed that an effective secondary nucleation over the surface of the developing crystals deposited onto the support was produced (Fig. 3d). After 6 h of treatment, an homogeneous

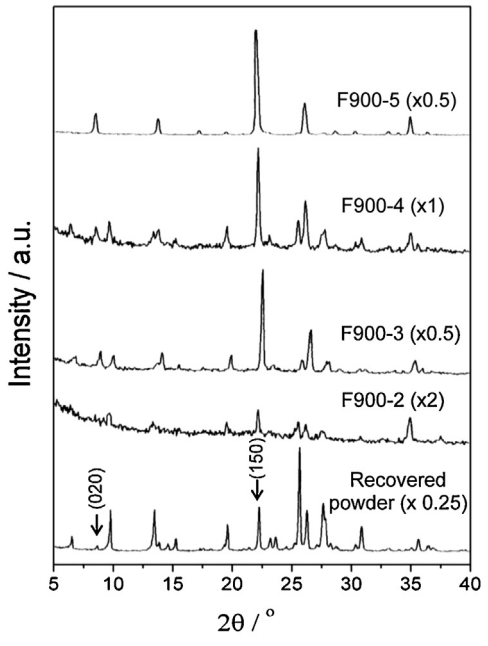

Fig. 2. XRD patterns of substrates pretreated at 900 °C (F900) and subjected to secondary synthesis.

mordenite film was developed, which covered the surface of the foil almost completely (Fig. 3b). In Fig. 3c, it can be seen that after 24 h the crystals in the film adopted an ordered geometry similar to the one reported in a previous work [14].

In the pioneering work of Jansen et al. [23], it was proposed that a zeolite film with crystallographic orientation can only be obtained if a gel layer is present on the surface of a support having a flat surface at nanometer scale. Consistent with this result, as shown in the image of Fig. 3c, a b-crystallographic orientation of the mordenite film was produced in which *b* planes were arranged parallel to the support surface. This was confirmed by the increase in the relative intensity of the diffraction signals of (0 2 0) and (1 5 0) planes, with respect to the same signals in the powder as shown in Fig. 2.

3.1.2. *Effect of the seed concentration*

In order to increase the zeolite loading and reduce the synthesis time, we increased the concentration of nanocrystals (Na-mordenite, Zeolyst) in the seeding solution to $10\,mg\,L^{-1}$. In the pictures of this sample after synthesis (Fig. 3f), a less homogeneous coating can be observed with overgrowths under the form of agglomerates deposited over a zeolite film developed on the support. Probably a fraction of the seeded crystals, which are anchored by weak forces of mechanical and Van der Waals type, detaches from the surface and migrates towards the solution during the synthesis, thus generating crystals within the solution that are afterwards randomly deposited. This is in agreement with the high crystallinity of the material recovered from the solution (shown in Fig. 2). In this vein, it has been reported that zeolite crystals physically deposited on a surface can move on it and migrate to the solution, provoking nucleation in the synthesis mixture [24]. Moreover, contrary to what was expected, the zeolite loading was lower (F900-4 in Table 1) mainly due to two reasons: the crystal growth within the solution was favored instead of the support and due to some detachment of the overgrowths during the ultrasonic cleaning.

In view of the results analyzed above, we performed seeding with a more diluted solution ($2\,g\,L^{-1}$). In this case, a higher mordenite loading was obtained (F900-5 in Table 1) achieving a film with a more homogeneous structure and a higher crystallographic orientation in the *b* axis (Fig. 2). Note that in this case, the signals from planes (2 0 0) and (2 0 2) at $2\theta = 9.8°$ and 25.7°, respectively, have almost disappeared whereas those of planes (0 2 0) at $2\theta = 8.7$ and (1 5 0) $2\theta = 22.3$ which characterize the b planes, have been intensified. This fact suggests that a lower number of nanocrystals on the foil surface probably decreases the amount of nanocrystals released to the solution promoting an ordered film growth onto the support to a greater extent. In view of the importance of the seeds concentration and their adherence onto the surface, experiments on FeCrAl alloy foils pre-treated with the cationic polymer PDDA were carried out.

3.2. *Synthesis of zeolite coatings on supports pretreated with PDDA*

We observed that the foils without thermal treatment are hydrophobic and the PDDA aqueous solution does not wet the surface correctly. Thus, the foils were treated at 700 °C during 1 h in order to generate an incipient smooth alumina layer without whiskers, which was actually obtained as shown in Fig. 5a. In this condition, the FeCralloy surface turned hydrophilic, allowing a homogeneous impregnation with the PDDA solution. The mordenite crystals dispersed in water had a negative net charge with a *z* potential of about −30 mV [25]. Consequently, the functionalization of the foils surface with the cationic polyelectrolyte would be beneficial for an electrostatic anchoring of the seeds. This procedure

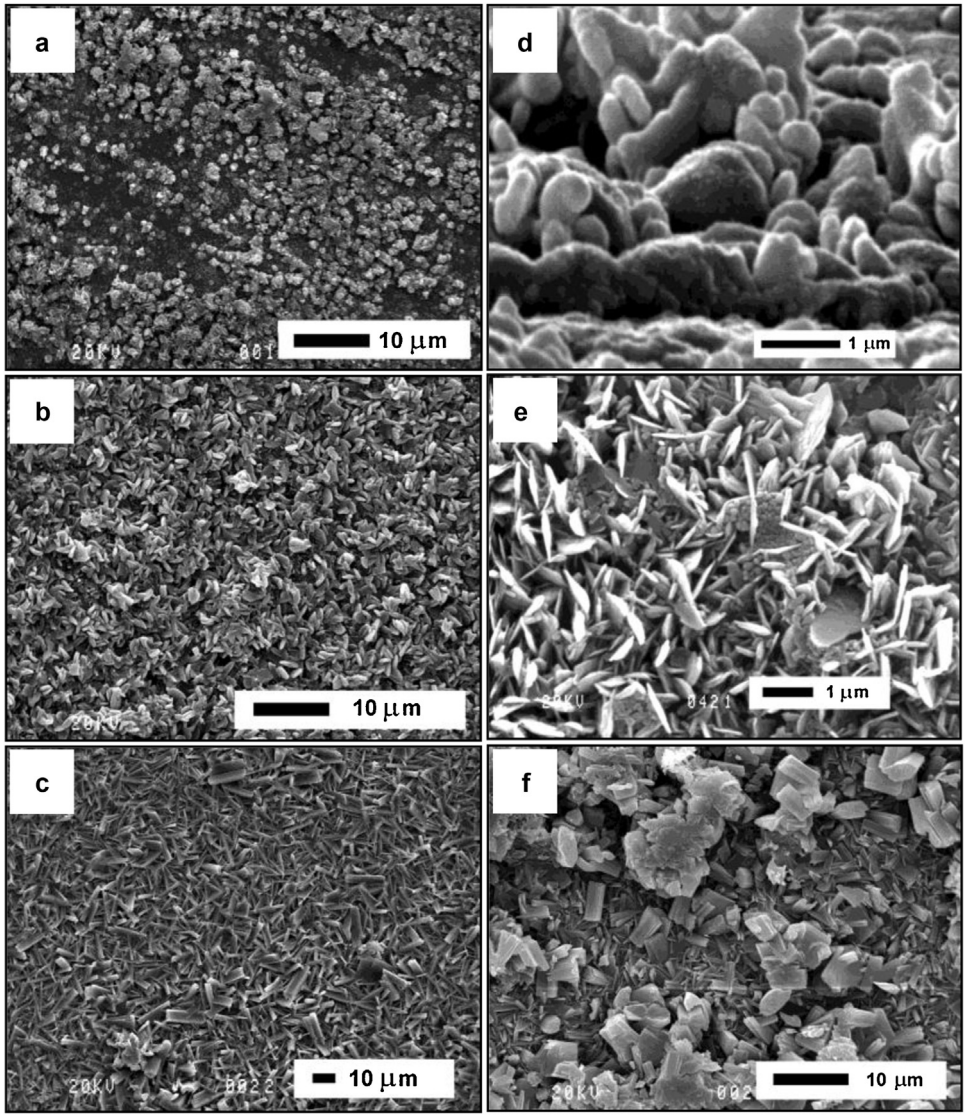

Fig. 3. Growths obtained onto foils pretreated at 900 °C and subjected to different syntheses conditions: (a) F900-1, (b) F900-2, (c) F900-3, (d) close view on sample F900-1, (e) seeding of nanocrystals on substrate with alumina whiskers and (f) F900-4.

of surface charge reversion has proved to be effective for the preparation of structured molecular sieve catalysts on various supports [26]. In this way, the foils calcined at 700 °C were treated with PDDA, put in contact with the seeding solution (Na-mordenite, Zeolyst, 5 g L t^{-1}) and then subjected to ultrasound for 1 min in water to remove loosely attached seeds. In Fig. 5a, it can be seen that a homogeneous distribution of nanocrystals over the entire surface was obtained, showing that the seeds remained firmly attached despite the ultrasound treatment and accounting for the seed-substrate strong interaction. The crystals cover the support completely, thus forming a monolayer; considering an average size of 200 nm, a density of around 25×10^{12} crystals cm^{-2} can be estimated. Afterwards, the seeded foils were hydrothermally treated varying synthesis time and seed concentration.

3.2.1. Temporal evolution of zeolite films

Table 2 summarizes the weight gains obtained under different conditions, which were in general higher than those obtained without PDDA. Although not detected by XRD, the SEM images show that a denser incipient growth was produced after 3 h of synthesis (Fig. 5b) if compared with that obtained without PDDA. After 6 h, the film crystallization evolved considerably (Fig. 5c and d). When synthesis was extended to 24 h, the films obtained showed a high crystallinity and a strong *b*-axis orientation (Fig. 5e and f) but non-desired agglomerates developed over the compact mordenite film which could negatively affect the flow patterns in the microreactor channels. The side views in Fig. 5 showed thicknesses of the films smaller than 1 μm, 3 μm and 12 μm for 3, 6 and 24 h of synthesis, respectively. In these syntheses, contrary to what was observed without PDDA, non-significant amounts of crystals developed within the solution (see Fig. 4), which is an important advantage and indicates a high affinity of the mordenite growth to the FeCralloy surface. This can be ascribed to the strong electrostatic forces generated between the polyelectrolyte with the seeded crystals and also probably with the nuclei generated in the gel film at the substrate-solution interphase during the hydrothermal synthesis.

3.2.2. Effect of seed concentration and synthesis gel dilution

Similarly to what was observed with the foils calcined at 900 °C, the increase of seed concentration (Na-mordenite, Zeolyst) resulted in a decrease in mordenite weight gain (Table 2) and also the growths presented agglomerates and overgrowths of similar aspect as those developed without PDDA. Taking into account this fact and the significant crystallization found in the solution, we inferred that

Table 2
Syntheses performed onto FeCralloy foils calcined at 700 °C and treated with PDDA.

Sample	Synthesis time (h)	Dilution ratio (H_2O:SiO_2)	Seeding suspension ($g\,L^{-1}$)	Weight gain (%)
F700-1	3	70:1.15	5	0.3
F700-2	6	70:1.15	5	3.8
F700-3	24	70:1.15	5	17.3
F700-4	24	70:1.15	10	9.7
F700-5	24	70:1.15	2	12.4
F700-6	24	35:1.15	2	28.2
F700-7	24	140:1.15	2	7.8
F700-8	24	210:1.15	2	3.7

Table 3
Physicochemical characteristics of the growths obtained employing seeding with different types of mordenite nanocrystals.

Crystal source	Continuity/crystal orientation	Weight gain (%)	EPMA zone	Si/Al	Cr/Al	Fe/Al
Na-mor Valfor	Continuous/b-oriented	14.7	Surface	8.30	0.20	0.50
			Middle	7.60	0.40	1.00
			Interphase	6.6	0.70	1.70
H-mor Zeolón	Discontinuous/azarous	10.6	Surface	7.18	0.18	0.45
			Middle	7.45	0.09	0.27
			Interphase	6.50	0.16	0.50
H-mor Dealum	Discontinuous/azarous	4.7	Surface	8.40	0.20	0.40
			Interphase	6.12	0.72	4.02

the agglomerates were formed in the vicinity of the interphase substrate-solution and then they precipitated onto the homogeneous film developed at the FeCralloy surface. On the contrary, when the seed concentration was lower (Table 2), the mordenite films were homogeneous with crystals of elongated shape without agglomerates and with a strong *b*-axis orientation (Fig. 5g).

The syntheses described above were performed with a gel with a H_2O:SiO_2 ratio of 70:1.15. Under the same seeding and hydrothermal conditions, the growth kinetics was modified using diluted and concentrated mixtures, keeping constant the ratios of the other reagents. When using a concentrated gel, an equivalent increase in the coating weight gain was found (Table 2), although the thickness was high and there were overgrowths (not shown). This is similar to what was found in the synthesis of zeolite films using concentrated synthesis mixtures in which non-epitaxial growths were produced [27]. Meanwhile, with a 140:1.15 dilution ratio the zeolite weight gain decreased (Table 2) and the XRD signal of the (0 0 2) planes increased, which indicated a change to a c-crystallographic orientation. Fig. 5h shows that crystals with the faces along the *c*-axis perpendicular to the support surface were developed. When a 210:1.15 H_2O:SiO_2 ratio was used, the amounts of reagents were not enough to develop a continuous coating.

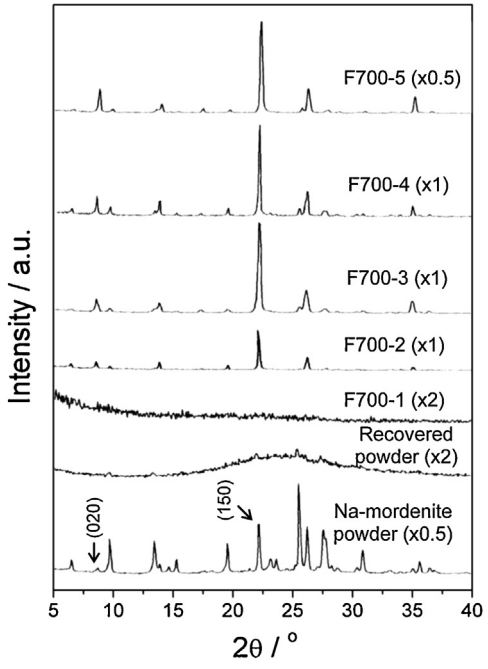

Fig. 4. XRD patterns of substrates pretreated at 700 °C (F700) and with PDDA subjected to synthesis.

3.2.3. *Effect of seeding with different commercial mordenite nanocrystals*

The syntheses described above were performed using nanocrystals from a Na-mordenite Zeolyst. In view of the strong incidence of the seeding step on the developed films, other types of commercial crystals were employed: another Na-mordenite and two H-mordenites. These syntheses were performed on foils treated with PDDA (F700). The seeding with crystals of Na-mordenite Valfor C500-11 yielded similar results as the ones previously discussed (Table 3), although in this case a stronger b-orientation and higher film homogeneity were produced (Fig. 6e and f). On the other hand, when both H-mordenite nanocrystals were used the weight gain was lower and uncovered zones with poor homogeneity were observed (Fig. 6a–d). Moreover, the XRD patterns of the powder recovered from these synthesis showed good crystallinity, thus confirming the poor efficiency of these seeds for the coating procedure. These observations clearly show that seeds from different sources affect the development and the microstructure of the growths, which could be ascribed to different isoelectric points of the nanocrystals, thus yielding different seeded surface density and surface environment during the growing process.

The EPMA chemical analyses of the growths (Table 3) show that the Si/Al ratio was between 6.1 and 8.4. A partial dissolution of the substrate and of the alumina surface layer during the early stages of the synthesis was also verified in view of the high concentration of Fe, Cr and Al in the zone close to the support-zeolite interphase. Such partial dissolution was beneficial in terms of adhesion of the film, since it generated a transition zone at the interface, which

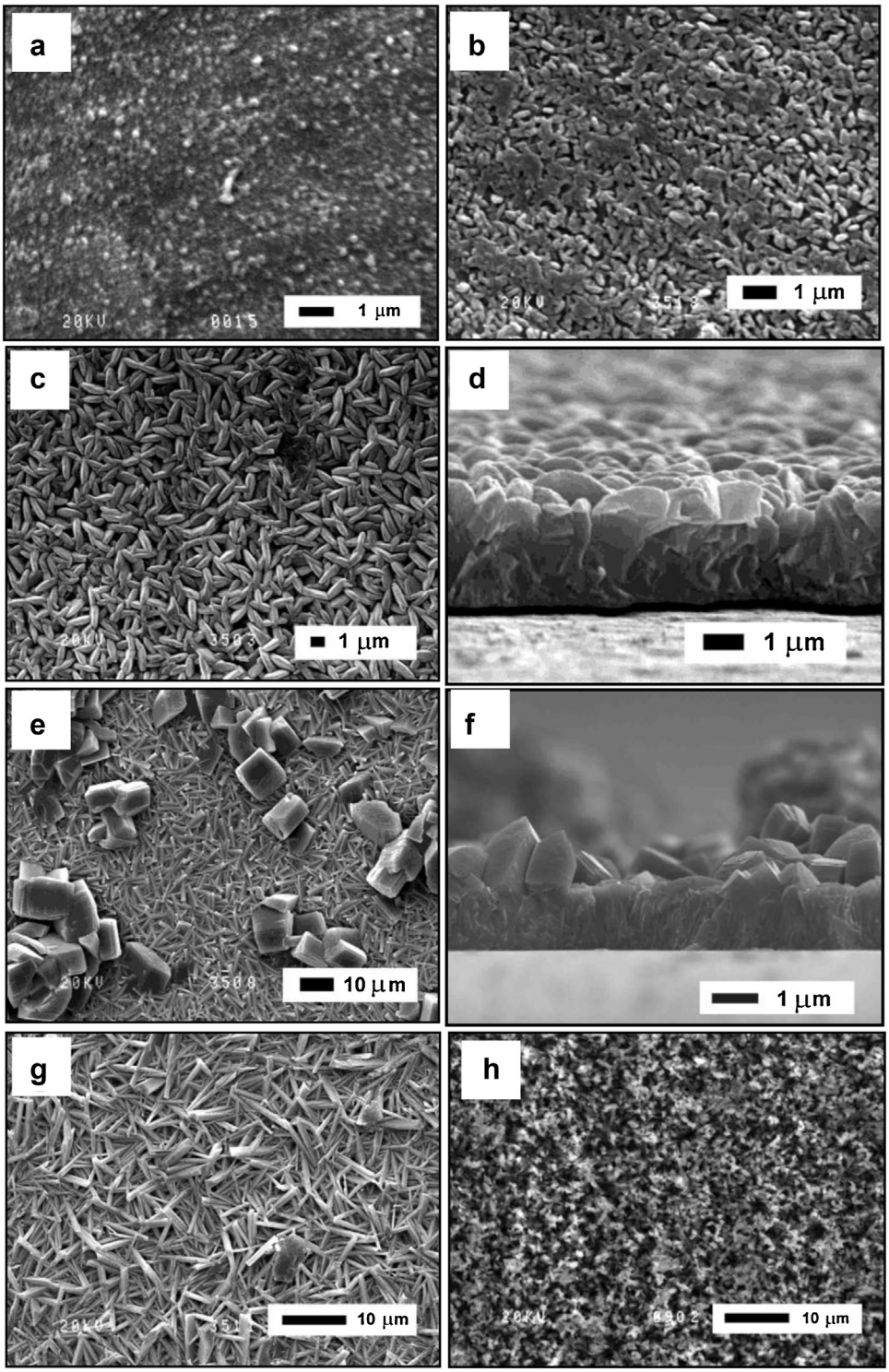

Fig. 5. Growths obtained onto foils pretreated at 700 °C and PDDA, subjected to different syntheses conditions: (a) pretreated FeCralloy surface with attached Na-mordenite seeds, (b) F700-1, (c) F700-2, (d) F700-2 side view, (e) F700-3, (f) F700-3 side view, (g) F700-5 and (h) F700-7. Before the observation, all samples were subjected to an ultrasonic treatment for 10 min. in water.

linked the support and the zeolite film. In fact, when all the growths obtained were subjected to ultrasound for 10 min. in water (see Section 2), they remained firmly attached as shown in Figs. 5 and 6, confirming their high adherence. Furthermore, there was no mass loss within the detection limit of the analytical balance, different from what happens with coatings of zeolites obtained by wash-coating. In such cases, it is common to observe mass loss after the ultrasound treatments [19].

3.3. Addition of Cu and Ce as active species

Taking into account the results discussed above, we selected the following preparation conditions that yielded b-oriented and very homogeneous films to coat microcorrugated foils: support calcination at 700 °C for 1 h, treatment with PDDA solution, seeding with a diluted suspension (1–2.5 mg L^{-1}) of Valfor C-50011 Na-mordenite nanocrystals, and finally a hydrothermal treatment for 24 h.

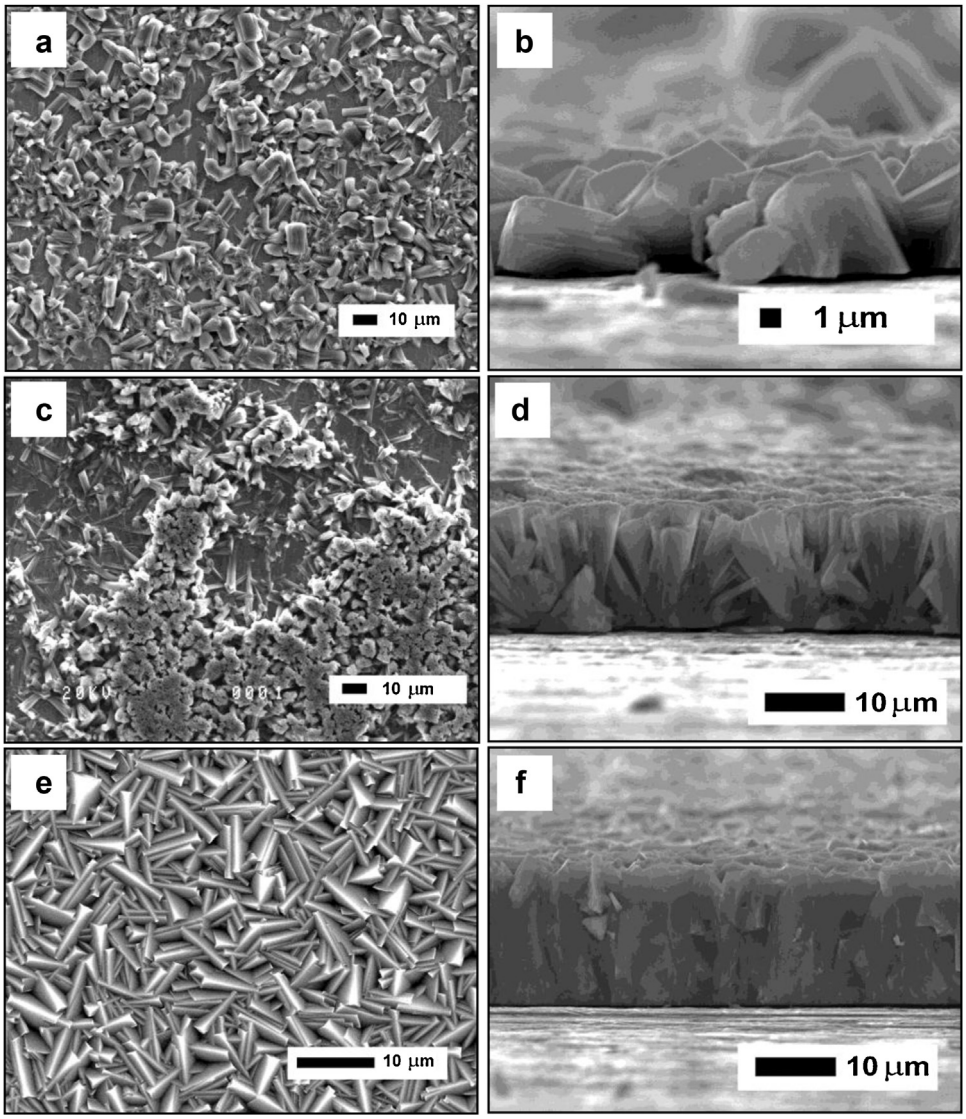

Fig. 6. Mordenite films obtained using different types of nanocrystals: (a) and (b) H-mor Zeolon, (b) and (c) H-mor dealuminated, (c) and (d) Na-mor Valfor C500-11.

After synthesis of the mordenite films, they were exchanged with Cu and impreganted with Ce as indicated in Section 2. We selected these active ingredients because there is a great interest in using catalysts based on more abundant and less expensive elements than noble metals. In fact, different catalyst formulations based on Cu and Ce oxides [28,29] have demonstrated a good catalytic performance for this reaction. To the best of our knowledge, only one study has been published on the use of Cu-zeolite as catalyst for the COProx reaction [30].

Table 4 shows the EPMA obtained at different points in the thickness of a Cu-exchanged film in a microchannelled foil. From the Cu/Al ratio, the Cu exchange level was estimated to be 60% of the C.E.C. which represents a 2 wt.% of Cu in the zeolite coating, the higher concentration of Cu being observed at the middle of the coating thickness. Other Cu-exchanged zeolite foils were impregnated with CeO_2 nanoparticles, with the purpose of generating a close interaction between Cu and Ce, which has been previously reported as beneficial for the CO oxidation activity.

In a sample obtained employing a 20 wt.% suspension of CeO_2, a high loading of about 30 wt.% CeO_2 with respect to the mass of mordenite coating in the microreactor was produced on the foil. This represents 6.10^{-4} mg of CeO_2/cm^2 of zeolite surface. In Fig. 7, it can be observed that CeO_2 patches of approximately 3 μm thickness covering the zeolite film were produced. Nowithstanding, the tortuous and open zeolitic film microstructure allowed the penetration of part of the Ce to internal zones of the growth, as determined by EPMA (Table 4). Furthermore, as mentioned above, a Fe and Cr concentration gradient was produced during the synthesis process, which increased towards areas close to the support. In other samples, the concentration of CeO_2 in the slurry was decreased up to 4 wt.%, and the impregnated foils were subsequently washed with distilled water in order to remove the excess of CeO_2. In this way, samples with dispersed CeO_2 nanoparticles were obtained with a CeO_2 loading of about 3 wt.% CeO_2 with respect to the mass of mordenite coating as determined gravimetrically. Although CeO_2 particles could not be detected by SEM, the absence of agglomerates indicates that a high dispersion was obtained.

3.4. CO oxidation in catalytic microreactors

Microreactors (MR) were assembled by stacking 5 micro-corrugated FeCralloy foils coated with Cu-mordenite or Cu,Ce/mordenite films between flat stainless steel plates. They were evaluated in the total CO oxidation as shown in Fig. 8. The Cu-mordenite microreactor evaluated at a 600 $cm^3\ min^{-1}\ g^{-1}$

Table 4
Elemental compositional profiles (EPMA) of mordenite films containing Cu and Ce.

Cu(2)-zeolite/FeCralloy foil	Si/Al	Cu/Al	Fe/Al	Cr/Al
(1) External zone	7.44	0.09	0.14	0.09
(2) External-middle zone	7.41	0.14	0.36	0.14
(3) Internal-middle zone	7.85	0.30	0.55	0.25
(4) Interfase zone	6.30	0.09	0.88	0.40
(5) Substrate (Fe,Cr,Al = 72,22,5)	0.21	–	9.57	3.43

Cu(2)–CeO_2(30)-zeolite/FeCralloy foil	Si/Al	Cu/Al	Ce/Al
(1) External zone	2.06	–	23.10
(2) Middle zone	6.78	0.16	3.44
(3) Interfase zone	4.68	0.09	1.13

Cu(2)–CeO_2(3)-zeolite/FeCralloy foil	Si/Al	Cu/Al	Ce/Al
(1) External zone	7.60	0.10	0.60
(2) External-middle zone	7.70	0.10	0.20
(3) Internal-middle zone	7.33	0.22	–
(4) Interfase zone	3.60	0.20	–

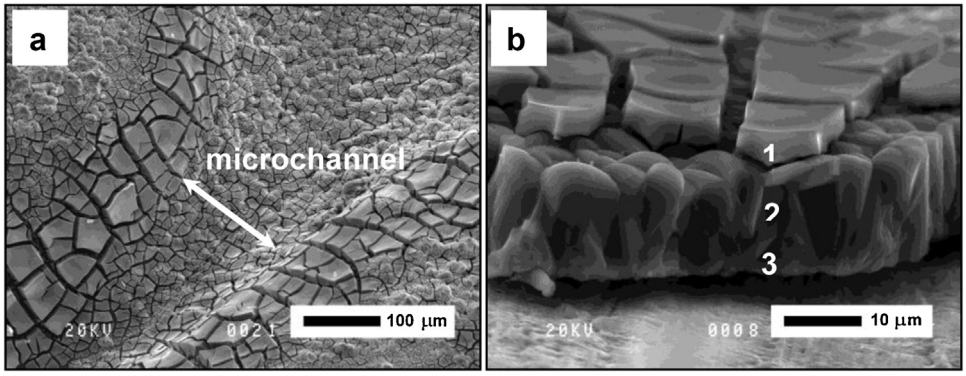

Fig. 7. Cu,Ce-mordenite catalytic film deposited onto a microcorrugated foil: (a) top view on the microchannel and (b) cross section of the film (the numbers indicate the zone of EPMA analyses).

flow/mass ratio (Cu(2)MR-a) with a feed composed of 1% CO and 2% O_2 showed 50% of conversion (T^{50}) at 320 °C. For the same microreactor, but with half the flow/mass ratio and 20% of O_2 in the feed gas (Cu(2)MR-b), the conversion curve shifted towards lower temperatures, reaching T^{50} at 289 °C, due to the combined effect of lower spatial velocity and higher oxygen concentration. The reaction rate, calculated at low conversion and assuming the behavior of a differential reactor, is the same under both conditions and similar to that obtained by Miró et al. [31] for powder Cu-mordenite, indicating that interfacial diffusion limitations are negligible.

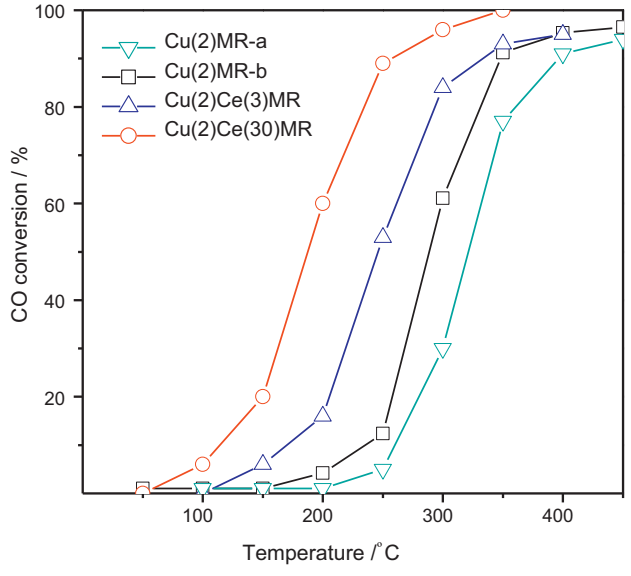

Fig. 8. CO conversion curves of Cu-mordenite/FeCralloy and Cu,Ce-mordenite/FeCralloy microreactors.

In the case of the microreactor formed with foils coated with Cu,Ce/mordenite films and containing 3 wt.% of CeO_2 (Cu(2)Ce(3)MR), which were evaluated under the same conditions shown above, the T^{50} was considerably lower (245 °C). This is a consequence of a close contact between Cu and Ce that promotes a catalytic synergic effect. As a matter of fact, it has been reported that the oxygen-enriched surface of CeO_2 located in the vicinity of Cu sites promotes the CO oxidation through a redox mechanism [32]. The possible influence of the Fe present in the coating, generated during the synthesis process, upon the CO conversion should not be excluded. In fact, Fe-zeolites have been reported as active materials for the reaction under study [33].

On the other hand the performance of the microreactor with a higher Ce content (Cu(2)Ce(30)MR), was notably superior, reaching T^{50} at 186 °C. This behavior not only indicates a good Ce–Cu contact but also an optimal Cu–Ce proportion, as already reported for this type of powder catalysts [34]. The performance (T^{50}) of the developed microreactors was comparable to that of CuO–CeO_2 bulk catalysts obtained by coprecipitation [34] and also to that of microreactors of CuO–Al_2O_3/stainless steel [35]. The excess of CeO_2 forming patches over the mordenite film does not contribute to the reaction but, probably, the small Cu–Ce particles located at the interstices formed between mordenite crystals are the effective active sites.

4. Conclusions

Microstructural properties of mordenite films obtained by secondary synthesis on micro-corrugated FeCralloy foils were optimized. Support calcination conditions, type and concentration of seeds in the seeding solution, synthesis gel dilution, and the functionalization of the FeCralloy surface with the cationic polyelectrolyte PDDA proved to have a strong impact on the regulation of the properties of the films. The generation of alumina whiskers in the support can serve to effectively anchor the seeds but through weak forces, causing them to become detached from the surface and migrate towards the solution during the synthesis, generating irregularly deposited cumulus. In contrast, a brief pretreatment of the foil at 700 °C developed a smooth hydrophilic alumina film allowing the adsorption of the cationic polymer PDDA which gives a better film quality and efficiency after the hydrothermal treatment. This is due to a more uniform seed coverage and a preferential crystal growth on the metallic surface, respectively. The latter is favored by the strong electrostatic forces generated between the polyelectrolyte and the seeded crystals and also probably by the nuclei generated in the gel film at the substrate-solution interphase during the film growth. Moreover, better homogeneity and optimal loadings were obtained using diluted seeding solutions of Na-mordenite nanocrystals instead of H-mordenite. In addition, it is convenient to use intermediate gel dilutions since more concentrated solutions decrease the homogeneity of the films and the efficiency of the growth on the surface, while more diluted gels alter the crystallographic orientation giving c-oriented growths.

We have demonstrated that films with optimal properties synthesized on micro-corrugated substrates and activated with Cu and Ce as active ingredients were successfully applied as microreactors for CO oxidation. The best results were obtained with microreactors prepared with films containing 2 wt.% of exchanged Cu and 30 wt.% of impregnated nano ceria.

Acknowledgments

The authors wish to acknowledge the financial support received from CONICET, ANPCyT and Universidad Nacional del Litoral. Thanks are also given to Elsa Grimaldi for the English language editing.

References

[1] L. Kiwi-Minsker, A. Renken, Catalysis Today 110 (2005) 2–14.
[2] G. Kolb, V. Hessel, Chemical Engineering Journal 98 (2004) 1–38.
[3] V. Sebastian, S. Irusta, R. Mallada, J. Santamaría, Catalysis Today 147S (2009) S10–S16.
[4] G. Kolb, V. Hessel, V. Cominos, C. Hofmann, H. Lowe, G. Nikolaidis, R. Zapf, A. Ziogas, E.R. Delsman, M.H.J.M. de Croon, J.C. Schouten, O. de la Iglesia, R. Mallada, J. Santamaria, Catalysis Today 120 (2007) 2–20.
[5] M.J.M. Mies, E.V. Rebrov, J.C. Jansen, M.H.J.M. de Croon, J.C. Schouten, Journal of Catalysis 247 (2007) 328–338.
[6] Y.S.S. Wan, J.L.H. Chau, K.L. Yeung, A. Gavriilidis, Journal of Catalysis 223 (2004) 241–249.
[7] N. Navascués, M. Escuin, Y. Rodas, S. Irusta, R. Mallada, J. Santamaría, Industrial and Engineering Chemistry Research 49 (2010) 6941–6947.
[8] W.N. Lau, K.L. Yeung, X.F. Zhang, R. Martin-Aranda, Studies in Surface Science and Catalysis 170 (2007) 1460–1465.
[9] K.L. Yeung, S.M. Kwan, W.N. Lau, Topics in Catalysis 52 (1/2) (2009) 101–110.
[10] M.J.M. Mies, E.V. Rebrov, C.J.B.U. Schiepers, M.H.J.M. de Croon, J.C. Schouten, Chemical Engineering Science 62 (2007) 5097–5101.
[11] J. Camra, E. Bielanska, A. Bernasik, K. Kowalski, M. Zimowska, A. Białas, M. Najbar, Catalysis Today 105 (3/4) (2006) 629–633.
[12] A. Eleta, P. Navarro, L. Costa, M. Montes, Microporous Mesoporous Materials 123 (2009) 113–122.
[13] E. Wloch, A. Lukaszczyk, Z. Zurek, B. Sulikowski, Catalysis Today 114 (2006) 231–236.
[14] J.M. Zamaro, M.A. Ulla, E.E. Miró, Applied Catalysis A: General 308 (2006) 161–171.
[15] J.M. Zamaro, M.A. Ulla, E.E. Miró, Microporous Mesoporous Materials 115 (2008) 113–122.
[16] J. Caro, M. Noack, P. Kolsch, R. Schafer, Microporous Mesoporous Materials 38 (2000) 3–24.
[17] G. Li, E. Kikuchi, M. Matsukata, Microporous Mesoporous Materials 62 (2003) 211–220.
[18] W. Maus, L. Wieres, US Patent 5,157,010 (1992).
[19] J.M. Zamaro, M.A. Ulla, E.E. Miró, Chemical Engineering Journal 106 (2005) 25–33.
[20] T. Nakazawa, M. Sadakata, T. Okubo, Microporous Mesoporous Materials 21 (1998) 325–332.
[21] G. Clet, J.A. Peters, H. van Bekkum, Langmuir 16 (2000) 3993–4000.
[22] K. Okamoto, H. Kita, K. Horii, K. Tanaka, Industrial and Engineering Chemistry Research 40 (2001) 163–175.
[23] J.C. Jansen, M. Stocker, H.G. Karge, J. Weitkamp, Studies in Surface Science and Catalysis 85 (1994) 215–250.
[24] A. Iwasaki, T. Sano, Y. Kiyozumi, Microporous Mesoporous Materials 38 (2000) 75–83.
[25] J.M. Zamaro, Ph.D. Thesis, School of Chemical Engineering (UNL), 2005.
[26] J. Sterte, J. Hedlund, D. Creaser, O. Ohrman, W. Zheng, M. Lassinantti, Q. Li, F. Jareman, Catalysis Today 69 (2001) 323–329.
[27] J.B. Loos, Zeolites 18 (1997) 278–281.
[28] P. Doggalia, S. Waghmarea, S. Rayalua, Y. Teraokab, N. Labhsetwar, Journal of Molecular Catalysis A: Chemical 347 (2011) 52–59.
[29] K.N. Rao, P. Bharali, G. Thrimurthulu, B.M. Reddy, Catalysis Communications 11 (2010) 863–866.
[30] T.R.O. Souza, A.J.S. Mascarenhas, H.M.C. Andrade, Reaction Kinetics and Catalysis Letters 87 (2006) 3–9.
[31] E.E. Miró, E.A. Lombardo, J.O. Petunchi, Journal of Catalysis 104 (1987) 176–185.
[32] A. Martínez-Arias, D. Gamarra, M. Fernández-García, X.Q. Wang, J.C. Hanson, J.A. Rodriguez, Journal of Catalysis 240 (2006) 1–7.
[33] J.O. Petunchi, W.K. Hall, Journal of Catalysis 78 (2) (1982) 327–340.
[34] M. Jobbágy, F. Mariño, B. Schonbrod, G. Baronetti, M. Laborde, Chemistry of Materials 18 (2006) 1945–1950.
[35] V. Snapkauskiene, V. Valincius, P. Valatkevicius, Catalysis Today 176 (2011) 77–80.